

# Off-axis PSF reconstruction for integral field spectrograph: instrumental aberrations and application to Keck/OSIRIS data

Anna Ciurlo<sup>a</sup>, Tuan Do<sup>a</sup>, Gunther Witzel<sup>a</sup>, Jessica Lu<sup>b</sup>, Jim Lyke<sup>c</sup>, Michael P. Fitzgerald<sup>a</sup>,  
Andrea Ghez<sup>a</sup>, Randy Campbell<sup>c</sup>, and Paolo Turri<sup>b</sup>

<sup>a</sup>University of California Los Angeles, 430 Portola Plaza, Los Angeles, CA 90095, USA

<sup>b</sup>University of California Berkeley, Campbell Hall, 501, Berkeley, CA 94720, USA

<sup>c</sup>W. M. Keck Observatory, 65-1120 Mamalahoa Hwy, Waimea, HI 96743, USA

## ABSTRACT

The integral field spectrograph OSIRIS at Keck I has been used to measure the motion of the stars around the supermassive black hole at the Center of the Galaxy. The small field of view provided and the crowding of the region prevent any good PSF estimate. A parallel imager can be used simultaneously to the IFU. However, its distance of 19 arcseconds prevents the observed PSF to be directly applied to the IFU because of anisoplanatism and instrumental aberrations. The Galactic Center Group at UCLA has developed an algorithms to predict PSF variability for Keck AO images (Off-axis PSF reconstruction, AIROPA software package). AIROPA allows us to use the parallel imager to correctly predict the IFU's PSF. We modified this package to adapt it to the case of OSIRIS imager and IFU (AIROPA-IFU) and characterized the instrumental aberrations of both detectors. Here, we present preliminary results of the application of this post-processing tool to OSIRIS datasets of the Galactic Center.

**Keywords:** Off-axis PSF Reconstruction, Field-dependent Aberrations, Integral Field Spectrograph, Keck Observatory, Keck I/OSIRIS, Near-infrared, Galactic center

## 1. INTRODUCTION

Integral field spectrographs (spectrograph equipped with integral field unit, IFU) are often coupled with adaptive optics (AO) systems on ground-based telescopes. Point-spread-function (PSF) information is central to extract science information but it is often difficult to obtain an accurate PSF estimate. This can be either because of the small field of view, the absence of any point-source (for example for extragalactic targets) or the crowding of the observed region. Crowding is the main cause preventing good PSF estimate at the Galactic Center. The Center of our Galaxy is an unique laboratory for the study of a supermassive black hole (SMBH) and its connection to galaxy evolution and formation. In particular, monitoring stars orbiting this SMBH gives a unique chance of testing General relativity in the strong gravity regime.<sup>1,2</sup> The Galactic Center Group at UCLA has been gathering data for over 20 years with this purpose. Such measurements are based on AO observations with the imager NIRC2 and the IFU OSIRIS<sup>3</sup> at Keck.

The OSIRIS<sup>4</sup> IFU's field of view is only 1-2 arcseconds for its smallest spatial scales (20 mas & 35 mas). Thus, there is often no good empirical PSF estimate since the PSF halo is larger than the field of view. The empirical PSF estimate is also difficult at larger scales in the very crowded innermost region of the Galactic Center (Fig. 1, right). OSIRIS is equipped with an larger field of view imager that can take parallel observations. This imager has been designed to track changes in the PSF of a reference star (Fig. 1, left). However the imager is 20 arcseconds away from the IFU, making it impossible to directly apply a PSF extracted on the imager onto the IFU data. This is due to atmospheric anisoplanatism and instrumental aberrations. For the imager,

---

Further author information:

A. Ciurlo: E-mail: ciurlo@astro.ucla.edu

T. Do: E-mail: tdo@astro.ucla.edu

anisoplanatism is particularly severe because it is far from the laser guide star (LGS), centered on the IFU, (Fig. 1).

The Galactic Center Group is developing a new software package to predict PSF variability for Keck AO images (Anisoplanatic and Instrumental Off-axis PSF Reconstruction, AIROPA<sup>5</sup>). The main goal of the project was to apply AIROPA to data taken with NIRC2 imager on Keck II.<sup>5-7</sup> The code requires two input models: a model describing the instrumental phase aberrations and an atmospheric model.

In this work, we show how we extended and adapted AIROPA for an IFU (AIROPA-IFU), specifically for case of OSIRIS. AIROPA-IFU enables us to derive the IFU's PSF from the off-axis imager PSF. To do so we use MASS/DIMM data to derive the atmospheric model of anisoplanatism and phase diversity data to characterize the instrumental aberrations of both the imager and the IFU's detectors. We present these changes and show preliminary results on LGS-AO to OSIRIS Galactic Center data. A more general and extensive presentation of the project, the need for this tool and the metrics we assume to test it are presented in Do *et al.* 2018 (these Proceedings).

In Section 2 we briefly describe the method used by AIROPA to predict off-axis PSFs and discuss the characterization of instrumental aberrations for both imager and spectrograph. In Section 3 we show how to apply AIROPA to an IFU, discuss the required wavelength sampling and present preliminary results of the application of AIROPA-IFU to OSIRIS Galactic Center data. In Section 4 we discuss the conclusions of this preliminary analysis.

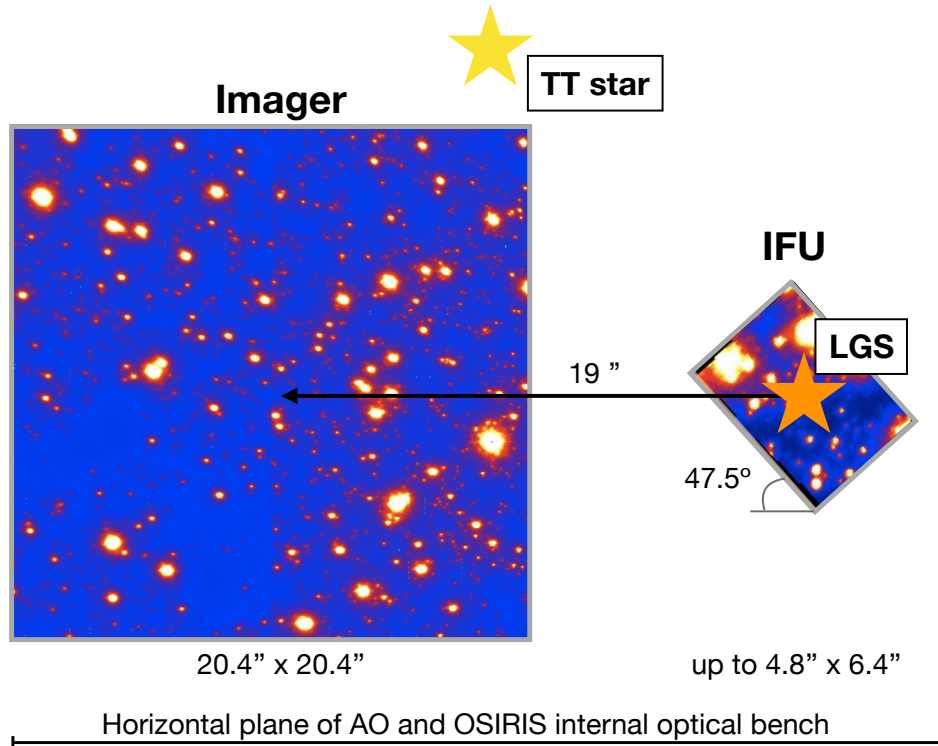


Figure 1. Representation of OSIRIS imager and spectrograph relative inclinations with an example of Galactic Center dataset.

## 2. AIROPA: OFF-AXIS PSF RECONSTRUCTION

### 2.1 AIROPA concept

AIROPA models the field-dependent PSF using two separable components that contribute to phase aberrations:

- 1 Instrumental phase aberrations – the phase aberrations due to non-common path aberrations, coming from the telescope and instruments. We use phase diversity data obtained with out-of-focus images of a fiber source onto the detector to produce phase maps (see Section 2.2).
- 2 Atmospheric effects – the aberrations coming from atmospheric phase errors and the cone effect due to single-conjugate LGS-AO. We use MASS/DIMM turbulence profiles independently recorded at the telescope site to estimate the long-exposure phase aberrations at different field positions.<sup>7,8</sup>

Once these two components are characterized, starting from an empirical on-axis PSF, the corrected PSF<sub>final</sub> can be written as:<sup>8,9</sup>

$$PSF_{final}(r) = PSF_0(r=0) \otimes PSF_{instr}(r) \otimes PSF_{atm}(r), \quad (1)$$

where  $PSF_0(r=0)$  is the empirical central PSF;  $PSF_{instr}(r)$  is estimated through a grid of phase maps in relation to the position on the detector ( $r$ );  $PSF_{atm}(r)$  is estimated with AIROPA atmospheric code.<sup>5-7</sup> This factorization allows to use the on-axis PSF<sub>0</sub> (with no anisoplanatism and no instrumental aberrations) as a reference for PSFs throughout the field of view (off-axis).

AIROPA has been applied to NIRC2 and is being tested with simulations and on-sky data (Witzel *et al.*, in prep.). This approach is very well suited to solve the OSIRIS PSF estimation problem: adapting AIROPA to OSIRIS allows to correctly make use of the imager that functions in parallel to the IFU.

## 2.2 Instrumental aberrations

We derived the phase aberrations as a function of field location using phase diversity data. These are obtained by taking a sequence of out-of focus images on the detector with a fiber light source. This measurement is repeated at several positions covering roughly the whole detector field resulting in a grid which samples the static instrumental aberrations (phase maps grid,<sup>6</sup> Witzel *et al.* in prep.).

For OSIRIS we characterized the instrumental aberrations of both the imager and IFU in the Spring of 2017. For the imager, we took a grid of nine by nine locations across the detector (see Fig. 2).

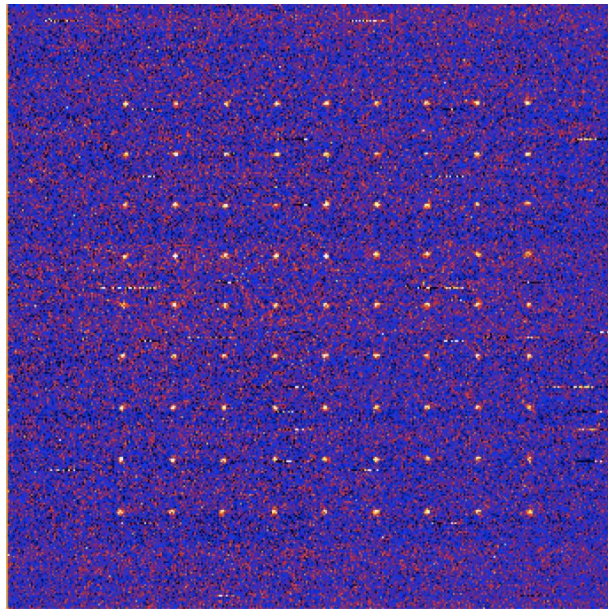


Figure 2. Grid of fiber images taken on OSIRIS imager showing the locations where the instrumental aberrations were mapped on the detector. The image show a superposition of all the in-focus fiber images.

At each detector position we took images at 2.5, -2.5 and -5 mm out-of-focus. The dataset is taken at 2.173  $\mu\text{m}$  and 20 mas plate scale. We made this measurements on the previous OSIRIS imager detector before

it was replaced at the end of 2017. The new detector is already in place and almost ready for use and we will be acquiring the same dataset in the near future to be able to characterize it.

For the IFU we only considered the central position since the field of view is small and we do not expect much variations. We took images at 2.2, -2.8 and -5.3 mm out-of-focus as shown in Fig. 3. We took the data at 20 mas platescale (the one usually used at Keck to do image sharpening procedure) and in Kn3 band (the preferred band for Galactic Center observations).

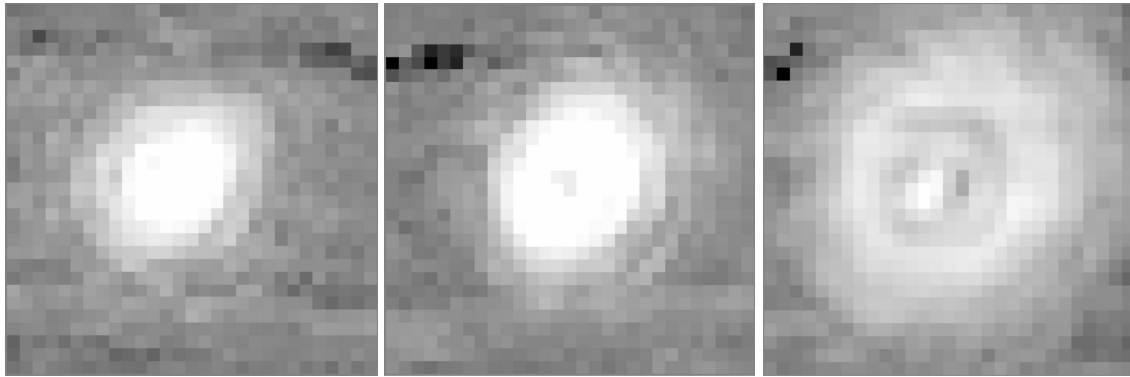


Figure 3. Phase diversity data on the OSRIIS IFU. Fiber images at 2.2 mm (*left*), -2.8 mm (*center*) and -5.3 mm (*right*) out-of-focus positions.

The phase diversity data is fed to a software that uses the Gerchberg-Saxton method,<sup>10</sup> an iterative algorithm for retrieving the phase. This is the same method used at Keck for image sharpening. The only differences are that we used higher signal-to-noise data, a larger number of iterations of the code, and more carefully used the random number generator.

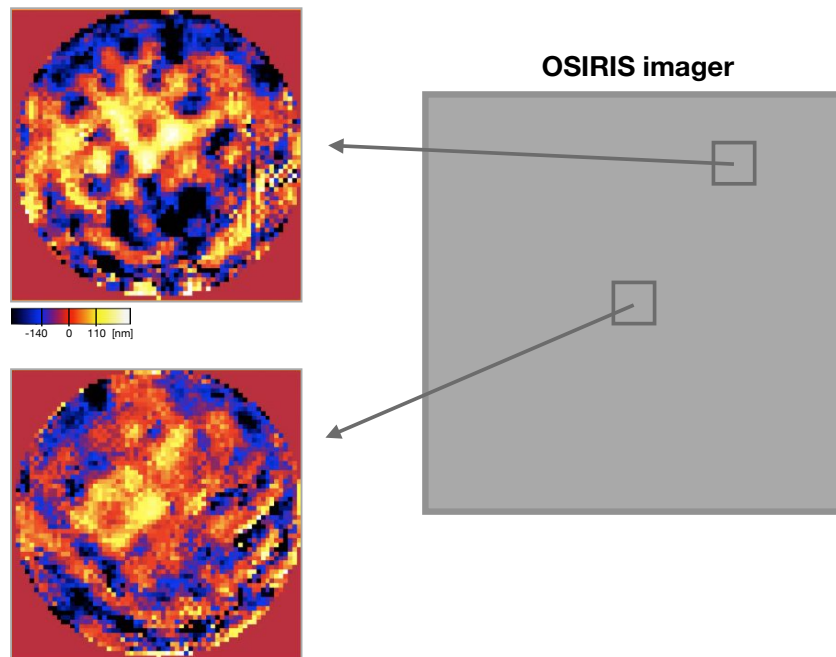


Figure 4. Examples of phase maps at different positions onto the imager detector of OSIRIS.

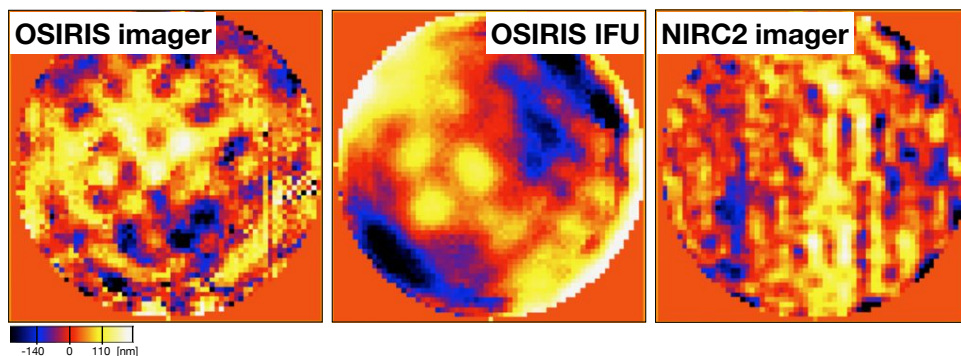


Figure 5. Phase maps at the OSIRIS imager’s upper-right corner (*left*) and at the IFU’s center (*center*). On the *right* NIRC2 central phase map is shown for comparison. All phase maps are show at the same scale and color-bar.

An example of two phase maps retrieved on the imager is shown in Fig. 4. The imager detector shows only small variations in phase aberrations across the detector.

The OSIRIS imager and IFU phase maps are compared to a phase map previously obtained on NIRC2 detector on Fig. 5. The wavefront errors of the three phase maps are compared in the following Table:

<i>Detector</i>	<i>RMS</i> [nm]
OSIRIS IFU	108
OSIRIS imager	87
NIRC2 imager	75

The OSIRIS IFU shows a much higher wavefront error that the other detectors, and an higher value than expected for the instrument. This might be due to the dataset and needs more investigation.

### 3. APPLICATION OF AIROPA TO AN INTEGRAL FIELD SPECTROGRAPH

With AIROPA-IFU the PSF observed on the imager can be used to predict the PSF on the IFU, taking into account both the atmospheric and instrumental effects: correction of the anisoplanatism for the imager, and correction of the instrumental aberrations for both.

#### 3.1 Procedure to predict the IFU’s PSF from imager

The procedure to obtain the IFU PSF starting from the imager involves several steps and can be briefly describes as follows:

- Several off-axis stars on the imager are used to construct an on-axis imager PSF (Fig. 6, top left).
- The imager PSF is rotated 47.5 degrees to take into account the respective orientation of imager and IFU (Fig. 6, top center).
- The rotated on-axis imager PSF is then converted to a given wavelength of the IFU spectral band (Fig. 6, top right).
- This PSF is then rescaled to the IFU pixel scale.
- The rescaled imager PSF, the MASS/DIMM data obtained the same night as the observations and the imager and IFU phase maps are fed to AIROPA-IFU to estimate the PSF on the IFU (Fig. 6, bottom right).

The same process can be repeated for any wavelength channel of the IFU. Fig 6 (bottom left and center) shows the predicted IFU PSF at two different wavelengths, as applied to Galactic Center data obtained in 2017.

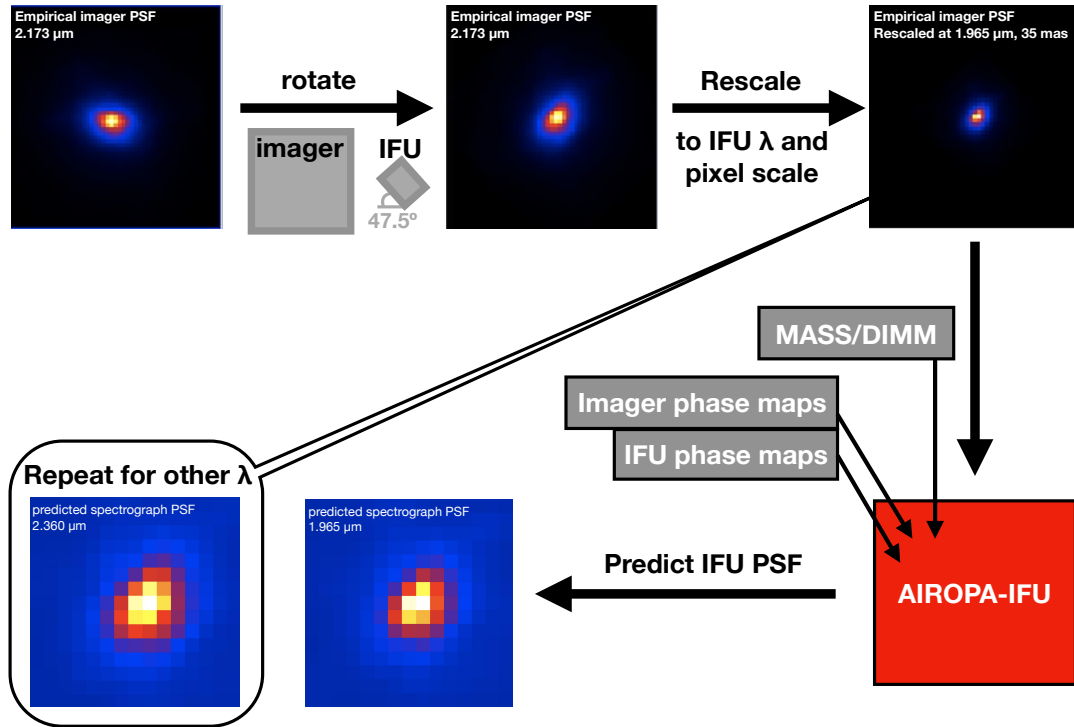


Figure 6. Simplified illustration of the procedure to apply AIROPA-IFU using 2017 Galactic Center data as an example.

### 3.2 Wavelength sampling

Predicting the IFU PSF requires the ability to predict the PSF at multiple wavelengths. The Kn3 band has 433 spectral channels, while Kbb band has 1665 (these are the filters most frequently used for Galactic Center observations). Running the algorithm over 1000 times is not very efficient. We investigated how fast the PSF changes for different spectral channels (taking into account diffraction and atmospheric effects) in Fig. 7. We

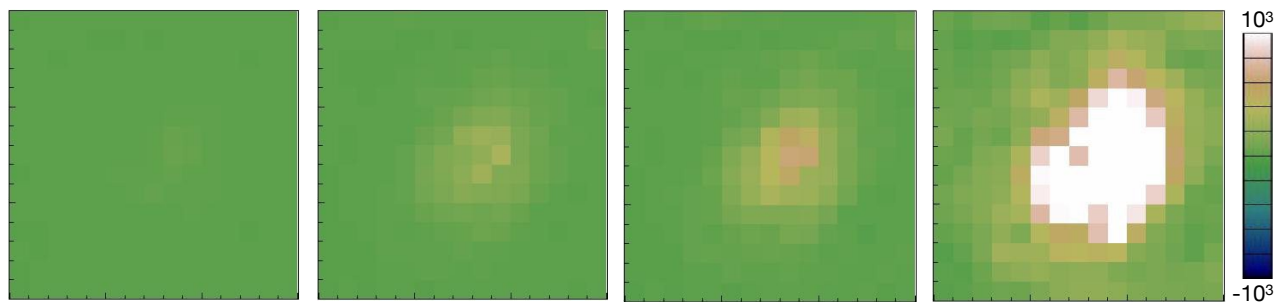


Figure 7. Residuals of IFU's PSF sampled at 10, 50, 100, or 1000 channels. All images are shown at the same scale and color-bar.

examined the difference between a PSF predicted at the first spectral channel of Kbb band and a PSF predicted 10, 50, 100 or 1000 channels away. Across 10 channels the PSF shows very little variation, across 100 channel the residuals start to show significant variations. We find that sampling every 50 channels seems to be sufficient to account for the PSF variation with the wavelength in this context.

### 3.3 Test AIROPA-IFU on Galactic Center datacube

We tested AIROPA-IFU on Galactic center data to evaluate its performance. In particular, we used data obtained with OSIRIS on May 18th, 2017. The IFU dataset has been acquired with 15 minutes exposures in 35 mas plate-scale and using the Kbb filter, which covers the wavelength range 1.965–2.381  $\mu\text{m}$ . The corresponding field of view is 0.665 x 2.24 arcseconds. The raw data were reduced with OSIRIS pipeline.<sup>11</sup> The parallel imager took 10 exposures of 2 seconds and 10 co-adds each, with the Kn3 filter. The imager pixel-scale is 20 mas. The 10 exposures were combined and the final field of view is 20.4 x 20.4 arcseconds.

The dataset is centered on a faint star S2-36,<sup>12</sup> located very close to a brighter star GCIRS16 CC. Due their proximity, S2-36 spectrum is dominated by GCIRS16 CC halo and it is very hard to extrapolate the fainter star spectrum without a good knowledge of the PSF halo. The standard procedure used to extract spectra in OSIRIS data is to simply use a circular aperture since we do not have any accurate knowledge of the PSF.

With AIROPA-IFU we address this problem and the parallel imager is used to predict the desired PSF. We apply the method as described in the above sections and use the predicted PSF to fit the IFU data (Fig 8, left) to model the observations (Fig 8, center). For comparison, we also fit the same data with a multiple 2D-Gaussians model without any knowledge of the PSF shape (Fig 8, right). The model obtained with the AIROPA-IFU well reproduces the observations: both stars are recovered, the PSF shapes are very consistent and have a well-reproduced cores. The 2D-Gaussian model is incapable of recovering the fainter star and is inadequate to describe AO data.

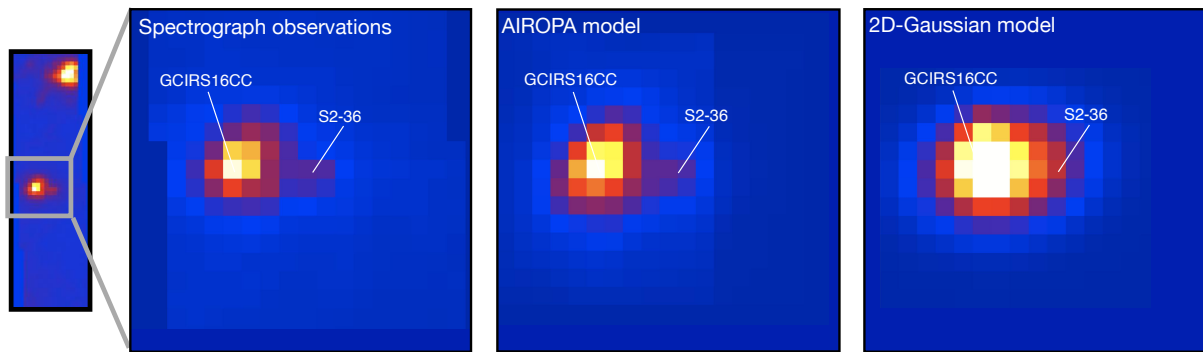


Figure 8. Application of predicted PSF to spectro-imaging data of two close stars at the Galactic center: spectroscopic observations (*left*) can be modeled through the AIROPA-predicted PSF (*center*) and compared to multiple 2D-Gaussians profile fit (*right*).

However, the S2-36 spectrum extracted with the newly predicted PSF is still dominated by the brighter star spectrum. We interpret this as an indication of the fact that the PSF model is still not perfect.

On the other hand, the spectral extraction is showing significant improvement for very bright stars. Fig. 9 (left) compares the spectrum of the brightest star in the field (GCIRS16 C) extracted with a circular aperture to the one extracted with the newly predicted AIROPA-IFU PSF. The signal-to-noise ratio improves of 50% when using AIROPA-IFU. On Fig. 9 (right) the same comparison is shown for the fainter star GCIRS16 CC. In this case the spectrum shows some unusual artifacts. This, together with the difficulty in recovering S2-36 spectrum, shows that the method still needs testing and refinement, especially for faint stars.

Some of the possible problems might reside in the IFU phase map that, as previously discussed, still need investigation. We will be acquiring a new dataset in the near future to assess whether the phase maps are accurate. There is also some uncertainty on the precise relative orientation of imager and spectrograph that we are currently addressing. The on-axis imager PSF extraction also need some refinement. Finally the code itself still needs some more testing and these are preliminary results. However the significant improvement in signal-to-noise ratio for the very bright star already shows the potential of this approach.

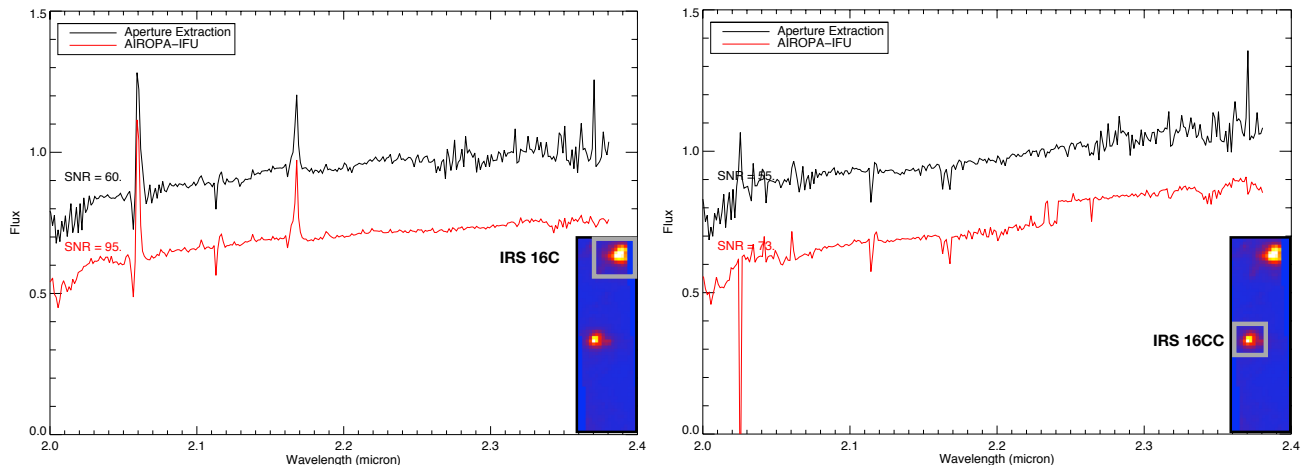


Figure 9. Comparison of star spectrum extracted with an aperture (*black*) and with the AIROPA-IFU predicted PSF (*red*) for a bright star (*left*) and a fainter one (*right*).

#### 4. CONCLUSIONS

We have adapted the AIROPA tool for off-axis PSF prediction for use with the Keck OSIRIS integral field spectrograph (AIROPA-IFU). We can predict the IFU PSF using simultaneous off-axis images of stars in a crowded field, together with a turbulence profile and phase maps characterizing both detectors used. The adaptation of AIROPA is still on-going, but preliminary results show that the predicted PSF is well matched to observations. With AIROPA the PSF core is well reproduced and the halo is better constrained even in crowded fields, such as the Galactic Center. The spectrum extraction in the case of very bright stars show an improvement of 50% in the signal-to-noise. Even though the code and the method still need improvement and testing these preliminary results show that there is great potential.

Knowledge of the halo of the IFU PSF will significantly improve the extraction of stellar spectra in crowded fields such as the Galactic center, or for high-contrast applications. The parallel imager corrected images can also open a new window to the use of imager and IFU in parallel, which was previously difficult to exploit without PSF reconstruction.

Finally, the generalization of AIROPA is a milestone on the way to implementing the semi-empirical off-axis PSF reconstruction approach to future instruments for extremely large telescopes such as the Thirty Meter Telescope (TMT).

#### REFERENCES

- [1] Zucker, S., Alexander, T., Gillessen, S., Eisenhauer, F., and Genzel, R., “Probing post-newtonian gravity near the galactic black hole with stellar doppler measurements,”
- [2] Hees, A., Do, T., Ghez, A. M., Martinez, G. D., Naoz, S., Becklin, E. E., Boehle, A., Chappell, S., Chu, D., Dehghanfar, A., Kosmo, K., Lu, J. R., Matthews, K., Morris, M. R., Sakai, S., Schödel, R., and Witzel, G., “Testing general relativity with stellar orbits around the supermassive black hole in our galactic center,” (05 2017).
- [3] Boehle, A., Ghez, A. M., Schödel, R., Meyer, L., Yelda, S., Albers, S., Martinez, G. D., Becklin, E. E., Do, T., Lu, J. R., Matthews, K., Morris, M. R., Sitarski, B., and Witzel, G., “An improved distance and mass estimate for sgr a\* from a multistar orbit analysis,” (07 2016).
- [4] Larkin, J., Barczyns, M., Krabbe, A., Adkins, S., Aliado, T., Amico, P., Brims, G., Campbell, R., Canfield, J., Gasaway, T., Honey, A., Iserlohe, C., Johnson, C., Kress, E., LaFreniere, D., Lyke, J., Magnone, K., Magnone, N., McElwain, M., Moon, J., Quirrenbach, A., Skulason, G., Song, I., Spencer, M., Weiss, J., and Wright, S., “OSIRIS: a diffraction limited integral field spectrograph for Keck,” in [*Society of Photo-Optical Instrumentation Engineers (SPIE) Conference Series*], Proc. SPIE **6269**, 62691A (June 2006).

- [5] Witzel, G., Lu, J. R., Ghez, A. M., Martinez, G. D., Fitzgerald, M. P., Britton, M., Sitarski, B. N., Do, T., Campbell, R. D., Service, M., Matthews, K., Morris, M. R., Becklin, E. E., Wizinowich, P. L., Ragland, S., Doppmann, G., Neyman, C., Lyke, J., Kassis, M., Rizzi, L., Lilley, S., and Rampy, R., “The AIROPA software package: milestones for testing general relativity in the strong gravity regime with AO,” in [*Adaptive Optics Systems V*], Proc. SPIE **9909**, 99091O (July 2016).
- [6] Sitarski, B. N., Witzel, G., Fitzgerald, M. P., Meyer, L., Ghez, A. M., Campbell, R. D., Lu, J. R., Matthews, K., Wizinowich, P., and Lyke, J., “Modeling instrumental field-dependent aberrations in the NIRC2 instrument on the Keck II telescope,” in [*Adaptive Optics Systems IV*], Proc. SPIE **9148**, 91486T (Aug. 2014).
- [7] Fitzgerald, M. P., Witzel, G., Britton, M. C., Ghez, A. M., Meyer, L., Sitarski, B. N., Cheng, C., Becklin, E. E., Campbell, R. D., Do, T., Lu, J. R., Matthews, K., Morris, M. R., Neyman, C. R., Tyler, G. A., Wizinowich, P. L., and Yelda, S., “Modeling anisoplanatism in the Keck II laser guide star AO system,” in [*Adaptive Optics Systems III*], Proc. SPIE **8447**, 844724 (July 2012).
- [8] Britton, M., “The anisoplanatic point spread function in adaptive optics,”
- [9] Fusco, T., Conan, J.-M., Mugnier, L. M., Michau, V., and Rousset, G., “Characterization of adaptive optics point spread function for anisoplanatic imaging. Application to stellar field deconvolution,” *A&AS* **142**, 149–156 (Feb. 2000).
- [10] Gerchberg, R. W. and Saxton, W. O., “A practical algorithm for the determination of the phase from image diffraction plane pictures,” *Optik* **35**, 237–250 (1972).
- [11] Lyke, J., Do, T., Boehle, A., Campbell, R., Chappell, S., Fitzgerald, M., Gasawy, T., Iserlohe, C., Krabbe, A., Larkin, J., Lockhard, K., Lu, J., Mieda, E., McElwain, M., Perrin, M., Rudy, A., Sitarski, B., Vayner, A., Walth, G., Weiss, J., Wizanski, T., and Wright, S., “OSIRIS Toolbox: OH-Suppressing InfraRed Imaging Spectrograph pipeline.” Astrophysics Source Code Library (Oct. 2017).
- [12] Do, T., Lu, J. R., Ghez, A. M., Morris, M. R., Yelda, S., Martinez, G. D., Wright, S. A., and Matthews, K., “Stellar Populations in the Central 0.5 pc of the Galaxy. I. A New Method for Constructing Luminosity Functions and Surface-density Profiles,” *ApJ* **764**, 154 (Feb. 2013).